



# CHORUS

This is the accepted manuscript made available via CHORUS. The article has been published as:

## Twin Higgs model with T parity

Jiang-Hao Yu

Phys. Rev. D **95**, 095028 — Published 30 May 2017

DOI: [10.1103/PhysRevD.95.095028](https://doi.org/10.1103/PhysRevD.95.095028)

# Twin Higgs With $\mathbb{T}$ Parity

Jiang-Hao Yu<sup>1,\*</sup>

<sup>1</sup>*Amherst Center for Fundamental Interactions, Department of Physics,  
University of Massachusetts-Amherst, Amherst, MA 01003, U.S.A.*

In twin Higgs models, a discrete  $\mathbb{Z}_2$  symmetry between the standard model Higgs and the twin Higgs is introduced to address the hierarchy problem. In this work, we propose another discrete symmetry in twin Higgs: the  $\mathbb{T}$  parity, which maps the twin Higgs quadruplet into its mirror copy. The  $\mathbb{T}$  parity brings us a whole group of  $\mathbb{T}$ -odd particles, and leads to a promising dark matter candidate. We present one realization of the  $\mathbb{T}$ -parity twin Higgs scenario by implementing the  $SU(2)_L \times SU(2)_R \times U(1)_1 \times U(1)_2$  gauge symmetry in the left-right twin Higgs model. In this specific setup, the  $\mathbb{T}$ -odd  $U(1)$  gauge boson could be the dark matter candidate, and the  $\mathbb{T}$ -odd particles have very distinct and interesting phenomenology.

## I. INTRODUCTION

In the standard model (SM), the large, quadratically divergent radiative corrections to the Higgs mass parameter destabilize the electroweak scale, which is known as hierarchy problem. The typical dynamical solution to this problem is to introduce a new symmetry which protects the Higgs mass against large radiative corrections. Under this direction are weak scale supersymmetry, composite Higgs and twin Higgs, etc. Recently the twin Higgs scenario [1, 2] attracts lots of attentions. And there have been studies on possible ultraviolet completion of the model [3–13] and on the twin particle phenomenology [14–17]. In these twin Higgs models, a twin Higgs doublet is introduced, and is mapped to the SM Higgs doublet through a discrete  $\mathbb{Z}_2$  symmetry. The  $\mathbb{Z}_2$  symmetry induces an accidental  $U(4)$  global symmetry in the Higgs sector, which ensures that the SM Higgs boson becomes pseudo-Goldstone boson of the global symmetry breaking. Therefore, the  $\mathbb{Z}_2$  symmetry in twin Higgs protects the Higgs mass against large radiative corrections. The twin Higgs scenario could be further classified by the gauge group in the models. Two kinds of gauge groups have been introduced: the mirror gauge group in the so-called mirror twin Higgs model [1, 6, 15], in which a mirror  $SU(3)'_c \times SU(2)'_L \times U(1)'$  symmetry is gauged, and the left-right gauge group in the left-right twin Higgs model [2], in which the SM gauge symmetry is extended to  $SU(3)_c \times SU(2)_L \times SU(2)_R \times U(1)$ .

Twin Higgs scenario not only addresses the hierarchy problem, but also provides rich cosmological implications [18–24], such as dark matter candidate, dark radiation, etc. To incorporate the dark matter candidate it is necessary to introduce a hidden sector in twin Higgs scenarios. In the mirror twin Higgs model [1, 6, 15], there is a hidden dark sector which is inherent in the model. The twin sector is only charged under new mirror SM gauge group and is connected to the SM sector via the  $\mathbb{Z}_2$  symmetry. Thus the twin particles are completely neutral under the SM gauge symmetry, and could only talk to

the SM sector through the Higgs boson. The twin particles in the mirror sector belong to a hidden dark sector, and it is the twin gauge symmetry that stabilizes the dark matter candidate. Similar dark matter candidate appears in the composite twin Higgs models, in which a twin QCD symmetry is introduced [8, 9]. Typically the dark matter candidate could be twin-neutrino, twin-onium, etc [18, 21, 23, 24]. It provides us very interesting cosmological consequence.

On the other hand, in the left-right twin Higgs model [2], there is no hidden dark sector contained in the model. In this model, both the SM color group and the  $U(1)$  group are not doubled by the  $\mathbb{Z}_2$  symmetry. Thus the twin particles in the twin sector could carry the SM color charge and the  $B - L$  charge. To incorporate hidden dark sector, the left-right twin Higgs model needs to be extended. Typical UV extensions of the left-right twin Higgs model are the composite twin Higgs with left-right symmetry and the supersymmetric twin Higgs with the left-right symmetry [3]. In the composite twin Higgs with left-right symmetry, such as Ref. [25], the hidden dark sector might or might not exist depending on the UV composite dynamics and the color and electroweak charge assignments of the twin particles. On the other hand, the supersymmetric twin Higgs with the left-right symmetry [3] contains the hidden sector: the sparticles in the mass spectra, which provide the dark matter candidate, the supersymmetric lightest sparticle. Thus its cosmological implications are quite similar to the typical supersymmetric dark matter.

In this work, we focus on the twin Higgs models with the left-right gauge symmetry. We propose a new way to introduce hidden dark sector and dark matter candidate in the left-right twin Higgs model, without the need of supersymmetric UV extension. In our setup, a discrete  $\mathbb{T}$  parity is introduced to obtain a hidden dark sector and thus the dark matter candidate. The  $\mathbb{T}$  parity has been introduced and investigated in the little Higgs model [26, 27], to avoid the tight constraints from electroweak precision tests and to introduce dark matter candidate in little Higgs. To be specific, we extend the left-right twin Higgs model in this work and impose the  $\mathbb{T}$  parity in this model. In our setup, two  $U(4)$  twin Higgs

---

\* jhyu@physics.umass.edu

quadruplets  $H_1$  and  $H_2$  are introduced, and an exchange symmetry in the Higgs sector is imposed:

$$\mathbb{T} \text{ parity : } H_1 = \begin{pmatrix} H_{1\text{SM}} \\ H_{1\text{twin}} \end{pmatrix} \leftrightarrow H_2 = \begin{pmatrix} H_{2\text{SM}} \\ H_{2\text{twin}} \end{pmatrix}, \quad (1)$$

The exchange symmetry between  $H_1$  and  $H_2$  is identified as the  $\mathbb{T}$ -parity. Under the  $\mathbb{T}$ -parity, one combination of the Higgs quadruplet is  $\mathbb{T}$ -odd, while another is  $\mathbb{T}$ -even. Not only the Higgs sector is doubled, the gauge and fermion structure could also be doubled through the  $\mathbb{T}$ -parity. Thus the  $\mathbb{T}$ -parity introduces a whole group of hidden particles, such as  $\mathbb{T}$ -odd Higgs,  $\mathbb{T}$ -odd top partner,  $\mathbb{T}$ -odd gauge boson, etc. Unlike the twin top partner is SM color neutral in mirror twin Higgs models, the  $\mathbb{T}$ -odd top partner carries the SM color. This leads to a different cosmological implications than the ones in the mirror twin Higgs. We present a realization of the  $\mathbb{T}$  parity left-right twin Higgs scenario by implementing the  $SU(2)_L \times SU(2)_R \times U(1)_1 \times U(1)_2$  gauge symmetry in twin Higgs model. In this setup, the  $\mathbb{T}$ -odd particles are the top partner  $T'$ , the  $\mathbb{T}$ -odd Higgs  $H'$ , and the  $\mathbb{T}$ -odd  $U(1)$  gauge boson  $B'$ , which is identified as the dark matter candidate. This  $\mathbb{T}$ -parity realization could be extended to other left-right twin Higgs models, such as composite twin Higgs with the left-right gauge symmetry.

The paper is organized as follows. In Section II we introduce the twin Higgs model with  $\mathbb{T}$ -parity, and then write down the Lagrangian for  $\mathbb{T}$ -even and -odd particles in Section III. Section IV discusses the twin Higgs mechanism. In Section V and VI we investigate the model constraints on the  $\mathbb{T}$ -even and -odd particles, respectively. Finally we conclude in Section VII.

## II. TWIN HIGGS MODEL WITH $\mathbb{T}$ -PARITY

We consider a two twin Higgs scenario, in which two  $U(4)$  invariant Higgs quadruplets are introduced:

$$H_1 \equiv \begin{pmatrix} H_{1L} \\ H_{1R} \end{pmatrix}, \quad H_2 \equiv \begin{pmatrix} H_{2L} \\ H_{2R} \end{pmatrix}. \quad (2)$$

The tree-level Higgs potential preserves an approximate global symmetry  $U(4)_1 \times U(4)_2$ :

$$V(H_1, H_2) = -\mu^2(|H_1|^2 + |H_2|^2) + \lambda[|H_1|^4 + |H_2|^4] \quad (3)$$

There are two discrete symmetries in the scalar potential:

- the  $\mathbb{Z}_2$  symmetry between  $H_L$  and  $H_R$ : it maps the twin Higgses into the SM Higgses:  $H_{1R} \xrightarrow{\mathbb{Z}_2} H_{1L}$ ,  $H_{2R} \xrightarrow{\mathbb{Z}_2} H_{2L}$ ;
- the  $\mathbb{T}$ -parity between  $H_1$  and  $H_2$ : it maps the two Higgs quadruplets into each other:  $H_1 \xrightarrow{\mathbb{T}} H_2$ .

The tree-level potential in Eq. 3 is invariant under both the  $\mathbb{Z}_2$  symmetry and the  $\mathbb{T}$ -parity. Because of the negative mass squared of the  $H_1$  and  $H_2$  in the tree-level

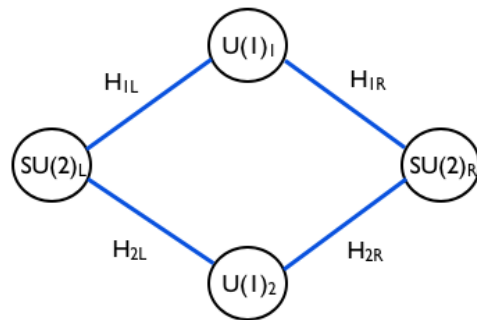


FIG. 1. The "Moose notation" [28] diagram of this model: the gauged symmetry  $SU(2)_L \times SU(2)_R \times U(1)_1 \times U(1)_2$  is represented by the solid circles, and the Higgs quadruplets  $H_1$  and  $H_2$  are represented by the links in between. The  $\mathbb{Z}_2$  symmetry acts as:  $H_{1L} \leftrightarrow H_{1R}$ ,  $H_{2L} \leftrightarrow H_{2R}$ ,  $SU(2)_L \leftrightarrow SU(2)_R$ . And the  $\mathbb{T}$ -parity acts as:  $H_{1L} \leftrightarrow H_{2L}$ ,  $H_{1R} \leftrightarrow H_{2R}$  and  $U(1)_1 \leftrightarrow U(1)_2$ .

potential, both the  $H_1$  and  $H_2$  develop vacuum expectation values (VEVs):

$$\langle h_{1L} \rangle^2 + \langle h_{1R} \rangle^2 = f^2/2, \quad \langle h_{2L} \rangle^2 + \langle h_{2R} \rangle^2 = f^2/2, \quad (4)$$

where  $f = \mu/\sqrt{\lambda}$ , and the  $h_{iL}$  and  $h_{iR}$  ( $i = 1, 2$ ) are the neutral components of the  $H_{iL}$  and  $H_{iR}$  in the quadruplet  $H_i$ , respectively. From Eq. 4, the VEVs ( $\langle h_{iL} \rangle$ ,  $\langle h_{iR} \rangle$ ) in the quadruplet  $H_i$  cannot be uniquely determined due to a residue  $U(1)_i$  symmetry in the tree-level potential. However, the tree-level potential receives additional corrections from the soft breaking term and radiative corrections, which will be discussed in detail in Sec. IV. Similar to the original twin Higgs [2], to obtain the correct Higgs boson mass, we introduce the soft  $\mathbb{Z}_2$  breaking but  $\mathbb{T}$ -parity invariant term

$$V_{\text{soft}} = m^2(H_{1L}^\dagger H_{1L} + H_{2L}^\dagger H_{2L}), \quad (5)$$

As additional benefit, this soft  $\mathbb{Z}_2$  breaking term breaks the residue  $U(1)_1 \times U(1)_2$  symmetry in the Higgs VEVs and thus uniquely determines the VEVs of ( $\langle h_{iL} \rangle$ ,  $\langle h_{iR} \rangle$ ):

$$\langle h_{1L} \rangle = \langle h_{2L} \rangle = 0, \quad \langle h_{1R} \rangle = \langle h_{2R} \rangle = f/\sqrt{2}. \quad (6)$$

Thus after the Higgses develop their VEVs, the  $\mathbb{T}$ -parity is still exact <sup>1</sup>.

<sup>1</sup> Because the gauge and fermion assignments shown in Tab. I respect the  $\mathbb{T}$ -parity, the radiatively corrections on the  $H_1$  terms and the  $H_2$  terms in the one-loop potential are the same, as discussed in Sec. IV. Thus including both soft breaking term and radiative corrections in the Higgs potential will only change the VEVs of the Higgses to obtain vacuum misalignment

$$\langle h_{1L} \rangle = \langle h_{2L} \rangle = v/\sqrt{2}, \quad \langle h_{1R} \rangle = \langle h_{2R} \rangle = f/\sqrt{2}, \quad (7)$$

and the  $\mathbb{T}$ -parity is still exact.

According to the potential in Eq. 3 and 5, the deepest minimum is developed at the VEVs:

$$\langle H_1 \rangle = \langle H_2 \rangle = \begin{pmatrix} 0 \\ 0 \\ 0 \\ \mu/\sqrt{2\lambda} \end{pmatrix} = \begin{pmatrix} 0 \\ 0 \\ 0 \\ f/\sqrt{2} \end{pmatrix}, \quad (8)$$

which break  $U(4)_V \rightarrow U(3)_V$  and leave  $U(4)_A$  unbroken. Here  $U(4)_V$  is the diagonal subgroup of  $U(4)_1 \times U(4)_2$ , and  $U(4)_A$  is the coset group. Therefore, the  $\mathbb{T}$ -parity is still exact after the global symmetry breaking  $U(4)_V \rightarrow U(3)_V$ . The  $U(4)_V$  is explicitly broken by gauging an  $SU(2)_L \times SU(2)_R \times U(1)_1 \times U(1)_2$  subgroup. Here  $H_{1L}$  and  $H_{2L}$  are doublets under the  $SU(2)_L$  gauge symmetry, while  $H_{1R}$  and  $H_{2R}$  are doublets under the  $SU(2)_R$  gauge symmetry. The  $H_1$  is only charged under  $U(1)_1$  gauge group, while the  $H_2$  is charged under  $U(1)_2$ . In terms of the "Moose notation" [28], we exhibit the Moose and linked fields in Fig. 1. Thus the two  $U(4)$  invariant Higgs fields have the following gauged Lagrangian:

$$\mathcal{L} = (D_\mu H_1)^\dagger D^\mu H_1 + (D_\mu H_2)^\dagger D^\mu H_2 - V(H_1, H_2). \quad (9)$$

The covariant derivatives are

$$\begin{aligned} D_\mu H_1 &= \partial_\mu H_1 + ig \mathbf{W}_\mu H_1 + ig' \mathbf{B}_{1\mu} H_1, \\ D_\mu H_2 &= \partial_\mu H_2 + ig \mathbf{W}_\mu H_2 + ig' \mathbf{B}_{2\mu} H_2, \end{aligned} \quad (10)$$

where

$$\mathbf{W}_\mu = \frac{1}{2} \begin{pmatrix} W_{L\mu}^a \tau^a & 0 \\ 0 & W_{R\mu}^a \tau^a \end{pmatrix}, \quad \mathbf{B}_{i\mu} = \frac{1}{2} \begin{pmatrix} B_{i\mu} & 0 \\ 0 & B_{i\mu} \end{pmatrix} \mathbf{1}$$

The gauged Lagrangian is invariant under the  $\mathbb{Z}_2$  mapping  $SU(2)_L \leftrightarrow SU(2)_R$ , and the  $\mathbb{T}$ -parity mapping:  $U(1)_1 \leftrightarrow U(1)_2$ .

	$SU(2)_L$	$U(1)_1$	$U(1)_2$	$SU(2)_R$
$H_{1L}$	<b>2</b>	$\frac{1}{2}$	0	<b>1</b>
$H_{1R}$	<b>1</b>	$\frac{1}{2}$	0	<b>2</b>
$H_{2L}$	<b>2</b>	0	$\frac{1}{2}$	<b>1</b>
$H_{2R}$	<b>1</b>	0	$\frac{1}{2}$	<b>2</b>
$q_L$	<b>2</b>	$\frac{1}{6}$	$\frac{1}{6}$	<b>1</b>
$q_R$	<b>1</b>	$\frac{1}{6}$	$\frac{1}{6}$	<b>2</b>
$\ell_L$	<b>2</b>	-1	-1	<b>1</b>
$\ell_R$	<b>1</b>	-1	-1	<b>2</b>
$T_{1L,R}$	<b>1</b>	$+\frac{2}{3}$	0	<b>1</b>
$T_{2L,R}$	<b>1</b>	0	$+\frac{2}{3}$	<b>1</b>

TABLE I. The particle contents and their quantum numbers in the model. Here  $T_1$  and  $T_2$  are new vector-like top singlets.

To generate the light Higgs boson mass without quadratic divergence, we introduce two vector-like top singlets:  $T_1$  and  $T_2$ . They are mapped into each other

under  $\mathbb{T}$ -parity:  $T_1 \leftrightarrow T_2$ . Adapting the matter contents in the left-right twin Higgs [2], we have the SM fermion contents (for simplicity, we only write down the third generation fermions) and the new fermions as follows:

$$\begin{aligned} q_L &= \begin{pmatrix} t_L \\ b_L \end{pmatrix}, \quad \ell_L = \begin{pmatrix} \nu_L \\ \tau_L \end{pmatrix}, \quad T_{1L}, T_{2L}, \\ q_R &= \begin{pmatrix} t_R \\ b_R \end{pmatrix}, \quad \ell_R = \begin{pmatrix} \nu_R \\ \tau_R \end{pmatrix}, \quad T_{1R}, T_{2R}. \end{aligned} \quad (12)$$

Their quantum number assignments are listed in Table I. The kinetic terms of the fermion Lagrangian are

$$\begin{aligned} \mathcal{L}_{\text{ferm}} &= \overline{q_{L,R}} \gamma^\mu D_\mu q_{L,R} + \overline{\ell_{L,R}} \gamma^\mu D_\mu \ell_{L,R} \\ &+ \overline{T_{1L,R}} \gamma^\mu D_\mu T_{1L,R} + \overline{T_{2L,R}} \gamma^\mu D_\mu T_{2L,R}, \end{aligned} \quad (13)$$

where

$$D^\mu T_{1,2} = \partial^\mu T_i + ig' Y B_{1,2}^\mu T_{1,2}, \quad (14)$$

$$\begin{aligned} D^\mu q_{L,R} &= \partial^\mu q_{L,R} + \frac{ig}{2} W_{L,R}^a \tau^a q_{L,R} \\ &+ ig' Y (B_1^\mu + B_2^\mu) q_{L,R}, \end{aligned} \quad (15)$$

$$\begin{aligned} D^\mu \ell_{L,R} &= \partial^\mu \ell_{L,R} + \frac{ig}{2} W_{L,R}^a \tau^a \ell_{L,R} \\ &+ ig' Y (B_1^\mu + B_2^\mu) \ell_{L,R}. \end{aligned} \quad (16)$$

The top quark sector contains the SM top quark and new vectorlike tops. The top Yukawa Lagrangian is

$$\begin{aligned} -\mathcal{L}_{\text{top}} &= y_{1L} \overline{Q}_L H_{1L} T_{1R} + y_{1R} \overline{Q}_R H_{1R} T_{1R} + M \overline{T}_{1L} T_{1R} \\ &+ y_{2L} \overline{Q}_L H_{2L} T_{2R} + y_{2R} \overline{Q}_R H_{2R} T_{2R} + M \overline{T}_{2L} T_{2R} + h.c. \end{aligned} \quad (17)$$

Due to the  $\mathbb{Z}_2$  symmetry and the  $\mathbb{T}$ -parity, we have  $y_{1L} = y_{2L} = y_{1R} = y_{2R} = y$ . We obtain the top Yukawa coupling and top quark mass from the top Yukawa Lagrangian. Without introducing any more extra matter fields, all other SM quarks and leptons can get their masses from the non-renormalizable terms

$$\begin{aligned} -\mathcal{L}_{\text{Yuk}} &= y_d \frac{\overline{q}_L H_{1L} H_{1R}^\dagger q_R + \overline{q}_L H_{2L} H_{2R}^\dagger q_R}{\Lambda} \\ &+ y_\ell \frac{\overline{\ell}_L H_{1L} H_{1R}^\dagger \ell_R + \overline{\ell}_L H_{2L} H_{2R}^\dagger \ell_R}{\Lambda} \\ &+ y_u \frac{\overline{q}_R H_{1R}^\dagger H_{1L} q_L + \overline{q}_R H_{2R}^\dagger H_{2L} q_L}{\Lambda} + h.c. \end{aligned} \quad (18)$$

Once the field  $H_{iR}$  acquires a VEV of order  $f$ , the non-renormalizable Lagrangian generates effective Yukawa couplings for the light quarks and leptons with the order of  $f/\Lambda$ , which is the typical size of the familiar Yukawa couplings in the SM [2]. In addition, we can write down the term

$$\frac{\overline{\ell}_R^C H_{1R} H_{1R}^C \ell_R + \overline{\ell}_R^C H_{2R} H_{2R}^C \ell_R}{\Lambda} \quad (19)$$

which generates large Majorana masses for the  $\nu_R$ :  $f^2/\Lambda$ . Thus the small neutrino masses could be obtained via the seesaw mechanism.

### III. T-EVEN/ODD LAGRANGIAN

The  $\mathbb{T}$ -parity is an exact symmetry of the Lagrangian. We could redefine the fields in the Lagrangian to have all the fields in the Lagrangian to be either  $\mathbb{T}$ -parity even or odd. We note that the fields  $W_{L,R}^\mu, q_{L,R}$  are  $\mathbb{T}$  even, but  $H_{1,2}, B_{1,2}^\mu, T_{1,2}$  are undetermined. Thus we define the following combinations:

$$\begin{aligned} H &= \frac{1}{\sqrt{2}}(H_1 + H_2), B^\mu = \frac{1}{\sqrt{2}}(B_1^\mu + B_2^\mu), \\ H' &= \frac{1}{\sqrt{2}}(H_1 - H_2), B'^\mu = \frac{1}{\sqrt{2}}(B_1^\mu - B_2^\mu), \\ T_{L,R} &= \frac{1}{\sqrt{2}}(T_{1L,R} + T_{2L,R}), \\ T'_{L,R} &= \frac{1}{\sqrt{2}}(T_{1L,R} - T_{2L,R}). \end{aligned} \quad (20)$$

Under these redefinition, we have

- $\mathbb{T}$ -parity even fields:  $H, B^\mu, T_{L,R}$ , and  $W_{L,R}^\mu, q_{L,R}$ ;
- $\mathbb{T}$ -parity odd fields:  $H', B'^\mu, T'$  with  $H' \leftrightarrow -H', B' \leftrightarrow -B', T' \leftrightarrow -T'$ .

Since the  $\mathbb{T}$ -parity is exact, it could be viewed as the origin of the dark matter symmetry, which could stabilize the dark matter candidate. Therefore, this model naturally explains the origin of the dark matter.

After field redefinitions, the two  $U(4)$  invariant quadruplets become

$$H \equiv \begin{pmatrix} H_L \\ H_R \end{pmatrix}, \quad H' \equiv \begin{pmatrix} H'_L \\ H'_2 \end{pmatrix}. \quad (21)$$

According to Eq. 8 and the  $\mathbb{T}$ -parity, the VEVs of the  $H$  and  $H'$  are

$$\begin{aligned} \langle H \rangle &= \frac{1}{\sqrt{2}}(\langle H_1 \rangle + \langle H_2 \rangle) = \begin{pmatrix} 0 \\ 0 \\ 0 \\ f \end{pmatrix}, \\ \langle H' \rangle &= \frac{1}{\sqrt{2}}(\langle H_1 \rangle - \langle H_2 \rangle) = 0. \end{aligned} \quad (22)$$

The  $\mathbb{T}$ -odd field  $H'$  has no VEV. Therefore, the global symmetry breaking is  $U(4) \rightarrow U(3)$  while  $U(4)'$  is unbroken. This can also be seen from the scalar potential for  $H$  and  $H'$ :

$$\begin{aligned} V(H, H') &= -\mu^2(|H|^2 + |H'|^2) \\ &\quad + \lambda[ (|H|^2 + |H'|^2)^2 + (H^\dagger H' + H'^\dagger H)^2 ]. \end{aligned} \quad (23)$$

The deepest minima of the potential exist at either  $(\langle H \rangle, \langle H' \rangle) = (f, 0)$  or  $(\langle H \rangle, \langle H' \rangle) = (0, f)$ .

The symmetry breaking pattern is

$$\begin{aligned} \text{global symmetry: } & U(4) \rightarrow U(3), \\ \text{gauge symmetry: } & SU(2)_L \times SU(2)_R \times U(1) \times U(1)' \\ & \rightarrow SU(2)_L \times U(1)_Y \times U(1)'. \end{aligned}$$

Let us parametrize the fields  $H$  nonlinearly in terms of the nonlinear sigma field

$$H = \exp \left[ \frac{i}{f} \begin{pmatrix} \mathbf{0}_{2 \times 2} & \mathbf{0}_{1 \times 2} & \mathbf{h} \\ \mathbf{0}_{2 \times 1} & 0 & C \\ \mathbf{h}^* & C^* & N \end{pmatrix} \right] \begin{pmatrix} \mathbf{0}_{1 \times 2} \\ 0 \\ f \end{pmatrix}, \quad (24)$$

where the field  $\mathbf{h}$  denotes the SM Higgs doublet  $\mathbf{h} = \begin{pmatrix} h^+ \\ h^0 \end{pmatrix}$ , and  $C^\pm$  and  $N$  are Goldstone bosons, which are absorbed by the  $SU(2)_R \times U(1)$  gauge bosons. Taking the expansion, the field  $H$  takes the form

$$H = \begin{pmatrix} f \frac{i\mathbf{h}}{\sqrt{\mathbf{h}^\dagger \mathbf{h}}} \sin\left(\frac{\sqrt{\mathbf{h}^\dagger \mathbf{h}}}{f}\right) \\ 0 \\ f \cos\left(\frac{\sqrt{\mathbf{h}^\dagger \mathbf{h}}}{f}\right) \end{pmatrix} \simeq \begin{pmatrix} i\mathbf{h} \\ 0 \\ f - \frac{1}{2f} \mathbf{h}^\dagger \mathbf{h} \end{pmatrix} \quad (25)$$

Here the field  $H$  plays the role of the twin Higgs as the original twin Higgs model. Another field  $H'$  does not obtain VEV, and thus it is just another scalar quadruplet in this model.

Using the redefined fields in Eq. 20, the kinetic Lagrangian in the scalar sector becomes

$$\begin{aligned} \mathcal{L} &= (D_\mu H^\dagger - ig' Y B'_\mu H'^\dagger)(D^\mu H + ig' Y B'_\mu H) \\ &\quad + (D_\mu H'^\dagger - ig' Y B'_\mu H'^\dagger)(D^\mu H' + ig' Y B'_\mu H), \end{aligned} \quad (26)$$

where the covariant derivative is defined as

$$\begin{aligned} D^\mu H &= \partial^\mu H + ig \mathbf{W}^\mu H + ig' \mathbf{B}^\mu H, \\ D^\mu H' &= \partial^\mu H' + ig \mathbf{W}^\mu H' + ig' \mathbf{B}^\mu H'. \end{aligned} \quad (27)$$

Note the Higgs mechanism for the  $\mathbb{T}$ -odd field  $B'^\mu$  is quite different from the typical case:

- In typical case, for example, the  $\mathbb{T}$ -even field  $B^\mu$  absorbs the CP odd component of the  $\mathbb{T}$ -even  $H$  and obtains its mass from its VEV  $\langle H \rangle$ ;
- In this model, the terms  $\partial^\mu H' B'_\mu H$  and  $B'^\mu B'_\mu H'^\dagger H$  in above Lagrangian indicate that the  $\mathbb{T}$ -odd field  $B'^\mu$  absorbs the CP odd component of the  $\mathbb{T}$ -odd  $H'$  but obtains its mass from VEV of the  $H$ .

The kinetic Lagrangian in the fermion sector becomes

$$\begin{aligned} \mathcal{L} &= \bar{T} i \gamma^\mu (\partial_\mu + ig' Y B_\mu) T + \bar{T}' i \gamma^\mu (\partial_\mu + ig' Y B_\mu) T' \\ &\quad - g' \bar{T} \gamma^\mu B'_\mu T' - g' \bar{T}' \gamma^\mu B'_\mu T. \end{aligned} \quad (28)$$

And the Yukawa Lagrangian in the top quark sector becomes

$$\begin{aligned} \mathcal{L}_{\text{Yuk}} = & \bar{q}_L H_L T_R + \bar{q}_R H_R T_L + M T_L T_R \\ & + \bar{q}_L H'_L T'_R + \bar{q}_R H'_R T'_L + M T'_L T'_R + h.c. \end{aligned} \quad (29)$$

We also obtain the Yukawa Lagrangian for the SM quarks and leptons:

$$\begin{aligned} -\mathcal{L}_{\text{Yuk}} = & \frac{y_d \bar{q}_L H_L H_R^\dagger q_R + y_\ell \bar{\ell}_L H_L H_R^\dagger \ell_R}{\Lambda} \\ & + y_u \frac{\bar{q}_R H_R^\dagger H_L q_L}{\Lambda} + h.c. \end{aligned} \quad (30)$$

#### IV. TWIN HIGGS MECHANISM

The gauge and Yukawa interactions break the global symmetry  $U(4)$  explicitly, generate masses for the Higgs boson, and trigger the electroweak symmetry breaking. We utilize the Coleman-Weinberg (CW) potential to quantify the radiative corrections of the Higgs potential. The one-loop CW potential in Landau gauge [29] is

$$\begin{aligned} V_{\text{CW}}(H) = & \frac{1}{64\pi^2} \text{STr} \left[ \Lambda^4 \left( \ln \Lambda^2 - \frac{3}{2} \right) + 2\mathcal{M}^2(H)\Lambda^2 \right. \\ & \left. + \mathcal{M}^4(H) \left( \ln \frac{\mathcal{M}^2(H)}{\Lambda^2} - \frac{3}{2} \right) \right], \end{aligned} \quad (31)$$

where the super-trace  $\text{STr}$  is taken among all the dynamical fields that have the Higgs dependent masses. The first term is the cosmological constant term, while the second term is responsible for the quadratic divergence of the Higgs boson masses. It is the third term that gives the scalar potential of the Higgs boson.

The Higgs-dependent charged gauge boson masses are

$$m_{W^\pm}^2 = \frac{1}{2} g_L^2 |H_L|^2, m_{W'}^2 = \frac{1}{2} g_R^2 |H_R|^2, \quad (32)$$

where  $g_L = g_R = g$  according to the  $\mathbb{Z}_2$  symmetry. The Higgs-dependent neutral gauge boson masses are

$$\begin{aligned} m_Z^2 & \simeq \frac{1}{2} (g^2 + g_Y^2) |H_L|^2 - \frac{1}{2f^2} \frac{g_Y^4}{g^2} |H_L|^4, \\ m_{Z'}^2 & \simeq \frac{1}{2} (g^2 + g'^2) f^2 - \frac{1}{2} (g^2 + g_Y^2) |H_L|^2 \\ & + \frac{1}{2f^2} \frac{g_Y^4}{g^2} |H_L|^4. \end{aligned} \quad (33)$$

The Higgs-dependent top quark masses are

$$\begin{aligned} m_t^2 & = \frac{y^4 |H_L|^2 |H_R|^2}{(M^2 + y^2 f^2)}, \\ m_{T'}^2 & = M^2 + y^2 f^2 - \frac{y^4 |H_L|^2 |H_R|^2}{(M^2 + y^2 f^2)}. \end{aligned} \quad (34)$$

For the  $\mathbb{T}$ -odd particles, we have

$$\begin{aligned} m_{B'}^2 & = \frac{1}{2} g'^2 (|H_L|^2 + |H_R|^2) = \frac{1}{2} g'^2 Y^2 f^2, \\ m_{T'}^2 & = M^2, \end{aligned} \quad (35)$$

which have no dependence on the Higgs boson field, and thus are not relevant to the Higgs boson mass and potential.

Let us first discuss the quadratic dependence of the Higgs boson in the CW potential in Eq. 31. Considering the contributions from the charged gauge bosons in Eq. 32, we have

$$V_{\text{CW}} \supset \frac{9\Lambda^2}{64\pi^2} (g_L^2 |H_L|^2 + g_R^2 |H_R|^2) \quad (36)$$

Only if the  $\mathbb{Z}_2$  symmetry is imposed ( $g_L = g_R = g$ ), there is no quadratic divergence on the Higgs boson mass from the charged gauge boson radiative corrections. Similarly, we obtain the CW potential from the neutral gauge bosons and the top quark sector

$$V_{\text{CW}} \supset \frac{9\Lambda^2}{64\pi^2} (m_Z^2 + m_{Z'}^2) \simeq \Lambda^2 f^2, \quad (37)$$

$$V_{\text{CW}} \supset -\frac{3\Lambda^2}{8\pi^2} (m_t^2 + m_{T'}^2) \simeq \Lambda^2 f^2. \quad (38)$$

In summary, the quadratic parts of the CW potential *accidentally* respect the original  $U(4)$  symmetry due to the  $\mathbb{Z}_2$  symmetry, which is the twin Higgs mechanism. Thus the Higgs mass does not receive any quadratic divergent contributions due to the twin Higgs mechanism.

Now let us analyse the radiatively generated Higgs potential. The leading Higgs potential is parametrized as

$$V(h^\dagger h) = a \sin^2 \left( \frac{\sqrt{h^\dagger h}}{f} \right) + b \sin^4 \left( \frac{\sqrt{h^\dagger h}}{f} \right), \quad (39)$$

where  $a$  and  $b$  are coefficients calculated from the one-loop CW potential. The gauge boson contributions are

$$\begin{aligned} a = & \frac{3}{64\pi^2} g^4 f^4 \left( \log \frac{\Lambda^2}{g^2 f^2/2} + 1 \right) \\ & + \frac{3g^2 (g^2 + 2g'^2) f^4}{128\pi^2} \left( \log \frac{\Lambda^2}{(g^2 + g'^2) f^2/2} + 1 \right), \quad (40) \\ b = & -a + \frac{3}{256\pi^2} (g^2 + g_Y^2) f^4 \left[ \log \frac{(g^2 + g'^2) f^2/2}{m_Z^2} - \frac{1}{2} \right], \end{aligned}$$

where  $m_Z^2 = \frac{1}{2} (g^2 + g_Y^2) f^2 \sin^2 x$  with  $x = v/f$ . Since  $a$  in above equation is positive, the gauge boson contributions could not trigger electroweak symmetry breaking. The top quark contributions are

$$\begin{aligned} a = & -\frac{3}{8\pi^2} y^4 f^4 \left( \log \frac{\Lambda^2}{M^2 + y^2 f^2} + 1 \right), \\ b = & -a + \frac{3y^4 f^4}{16\pi^2} \left[ \log \frac{M^2 + y^2 f^2}{m_t^2} - \frac{1}{2} \right], \end{aligned} \quad (41)$$

where the top-Yukawa coupling is defined as  $y_t = y \frac{yf}{\sqrt{M^2 + y^2 f^2}}$ , and  $m_t^2 = y_t^2 f^2 \sin^2 x$ . Therefore, the electroweak symmetry breaking is triggered by the top quark contributions. The Higgs boson mass is calculated via

$$m_{\text{Higgs}}^2 \simeq -\frac{a}{b} f^2, \quad (42)$$

But here we have  $a \sim b$ , and thus we obtain the Higgs mass is around  $f^2$ , which is too heavy. We need to add soft mass term, which only break the  $\mathbb{Z}_2$  symmetry softly but the  $\mathbb{T}$ -parity is still exact. The soft  $\mathbb{Z}_2$  breaking term in Eq. 5 reads

$$V_{\text{soft}} = m^2(H_{1L}^\dagger H_{1L} + H_{2L}^\dagger H_{2L}). \quad (43)$$

The Higgs mass is then

$$m_{\text{Higgs}}^2 \simeq \frac{a - m^2 f^2}{b} f^2. \quad (44)$$

Since the Higgs mass is measured to be 125 GeV, we could determine the soft mass parameter  $m^2$  once we know the new physics scale  $f$ . Furthermore, given various radiative corrections, we could estimate the fine-tuning by considering the following mass ratio

$$\Delta_m = \left| \frac{2\delta m}{m_h^2} \right|^{-1} \simeq \frac{m_h^2}{2|a|}. \quad (45)$$

Once we know the scale  $f$ , we could estimate the level of tuning in this model.

The  $\mathbb{T}$ -odd Higgs quadruplet  $H'$  also receives radiative corrections. Let us denote component fields in the  $H'$  as

$$H' = \begin{pmatrix} H'_L{}^+ \\ H'_L{}^0 + iA'_L{}^0 \\ H'_R{}^+ \\ H'_R{}^0 + iA'_R{}^0 \end{pmatrix}. \quad (46)$$

Due to the exact  $\mathbb{T}$ -parity, although the  $H'$  does not mix with the  $H$ , they share the same potential, as shown in Eq. 24. Therefore, at tree-level, after the  $H$  obtains its VEV  $\langle H_L \rangle = f \sin \frac{v}{f}$ ,  $\langle H_R \rangle = f \cos \frac{v}{f}$ , we obtain the tree-level masses

$$m_{H'_L{}^0}^2 = 2\lambda f^2 \sin^2 \frac{v}{f}, \quad (47)$$

$$m_{H'_R{}^0}^2 = 2\lambda f^2 \cos^2 \frac{v}{f}, \quad (48)$$

while other components are massless. On the other hand, since  $H'$  has no VEV at all <sup>2</sup>, all the components receive radiative corrections in addition to the tree-level masses:

$$m_{\text{all } H' \text{ components}}^2 \simeq \frac{1}{16\pi^2} g^4 f^2 \log \frac{\Lambda}{f}. \quad (49)$$

Similar to radiative corrections, adding soft mass terms will also lift the masses of the  $H'$  component fields. Given the soft mass terms in Eq. 43, all  $H'_L$  component fields obtain additional mass corrections:

$$m_{\text{all } H'_L \text{ components}}^2 \simeq m^2. \quad (50)$$

If we add soft mass terms for the  $H'_R$ , all the  $H'_R$  component fields will also receive corrections from the soft term. Therefore, the masses of the  $H'$  components will be the sum of all kinds of mass corrections. Since the soft mass terms origin from the ultraviolet physics, the masses of the  $H'$  component fields should be quite sensitive to the UV completion of this model.

## V. MODEL CONSTRAINTS

The strongest experimental constraints on the model come from direct searches at the LHC on the new  $\mathbb{T}$ -even particles: the new gauge bosons  $W'$ ,  $Z'$  and the colored heavy top  $T$ . Both ATLAS and CMS investigated the exotic  $W'$ ,  $Z'$ ,  $T'$  resonances. The latest experimental bounds on masses of these resonances are summarized as follow:

- If the right-handed  $W'$  decays to right-handed neutrino and lepton, the high mass resonance searches in the lepton plus transverse missing energy final states put strong constraint on the  $W'$  mass. In our setup, the right-handed neutrino masses are around the scale  $f$ , which is the see-saw mechanism to generate the neutrino mass. Therefore, the right-handed  $W'$  will dominantly decay to di-jet and single top final states. Due to huge QCD backgrounds in di-jet channel, we expect that the single top final states provide us the tightest constraint on the  $W'$  mass. Based on the 13 TeV CMS data with  $12.9 \text{ fb}^{-1}$  luminosity [32], the observed limits on the right-handed  $W'$  at 95% confidence level (CL) is  $m_{W'} > 2.6 \text{ TeV}$  <sup>3</sup>. But this is for the right-handed  $W'$  with 100% decay branching ratio to single top. Recasting the updated exclusion limit with branching ratios, we obtain  $m_{W'} > 1.67 \text{ TeV}$ .
- The dileptonic final states at the LHC put the strongest limit on the  $Z'$  gauge boson. Based on the 13 TeV ATLAS ( $13.9 \text{ fb}^{-1}$ ) [35] and CMS ( $2.9 \text{ fb}^{-1}$ ) [34] data, the observed limits on the sequential  $Z'$  is  $m_{Z'} > 4.05 \text{ TeV}$  at 95% CL. Taking into account branching ratio of the dilepton final state (around 2.5% in this model), we obtain the exclusion limit  $m_{Z'} > 2.56 \text{ TeV}$  in our setup.
- The heavy top quark partner  $T$  has been investigated at both the ATLAS [36] and CMS [37]. The tightest constraint on  $T$  come from combining the exclusion limits in the decay channels  $T \rightarrow tZ$ ,  $T \rightarrow bW$  and  $T \rightarrow th$ . Based on the ATLAS data

<sup>2</sup> It is different from the case that  $H'$  obtains its VEV [2, 30]. If the  $H'$  has VEV  $\langle H'_R \rangle = f'$ , the CP-odd scalar in  $H'_R$  will be massless due to a global residue  $U(1)_R$  symmetry.

<sup>3</sup> The exclusion limit from ATLAS [33] are slightly weaker because 8 TeV data was used in their analysis. Furthermore, flavor physics, such as the  $K_S - K_L$  mixing, etc, also put constraint on the  $W'$  mass, but it is weaker than the latest LHC constraints.

with  $11.5 \text{ fb}^{-1}$  luminosity at 13 TeV [36], the updated exclusion limit is around 850 GeV after taking the branching ratios into account.

From above, we find that the tightest constraint comes from the  $Z'$  dileptonic searches. Converting to constraints on the scale  $f$ , we obtain that the scale  $f > 4.8$  TeV. This introduces a tuning between the scale  $f$  and the electroweak scale, which is the so-called little hierarchy problem. Note that mass bounds on  $T$  is not so tight, because both the parameter  $M$  and the scale  $f$  contribute to the  $T$  mass. The vectorlike mass  $M$  lifts the  $T$  mass and could keep the scale  $f$  below 700 GeV. We could utilize similar setup to lift the masses of the new gauge bosons while keep the scale  $f$  below 1 TeV. Furthermore, lifting the new gauge boson masses will also help escape the indirect limits from electroweak precision tests. If the masses of the  $W'$  and  $Z'$  are not so heavy, the electroweak precision data put strong constraints on the model parameters [38]. However, when the gauge boson masses are heavier than 2 TeV, the electroweak precision constraints could be much weaker<sup>4</sup>

There are ways to lift the new gauge boson masses. Typically we introduce new scalar fields which are charged under the gauge group of the model. To keep other sectors in this model unaffected, we need to assign such new scalar fields only play the role of giving the new gauge boson masses without interacting with other fermions or scalars. Here we suggest two ways to lift the gauge boson masses:

- way I: introduce additional complex scalar  $S$ , which is only charged under  $U(1)_1$  and  $U(1)_2$ . The same  $U(1)$  charges are needed to keep the  $\mathbb{T}$ -parity exact. After this new scalar  $S$  obtains its VEV  $f'$ , the  $\mathbb{T}$ -even gauge boson  $Z'$  obtains its mass of order  $\sqrt{f^2 + f'^2}$ . In this way, the bound on the scale  $f$  could be relaxed and thus the tight constraints from the dileptonic  $Z'$  searches can be avoid. We could lower the scale  $f$  to be around 2 TeV in which the  $W'$  mass bound plays the significant role.
- way II: introduce additional Higgs quadruplet  $\tilde{H}$ , which is charged under  $SU(2)_L \times SU(2)_R$  and  $U(1)_1 \times U(1)_2$ . Similarly, the same  $SU(2)$  and  $U(1)$  charges are needed to keep the  $\mathbb{T}$ -parity exact. After the Higgs quadruplet  $\tilde{H}$  obtains its VEV  $f'$ , both the  $W'$  and  $Z'$  obtains their masses of order  $\sqrt{f^2 + f'^2}$ . In this way, we could lift the masses of the  $W'$  and  $Z'$  while keeping the  $f$  to be around 1 TeV.

Therefore, although the current limits on the  $W'$  and  $Z'$  are tight, the scale  $f$  could still be around TeV scale. Furthermore, if we assume the new scalar masses are heavier

than TeV scale by introducing soft mass terms, adding these new scalars will not affect the phenomenology below TeV scale. We will simply assume these new scalars are very heavy and only affect the  $W'$  and  $Z'$  masses.

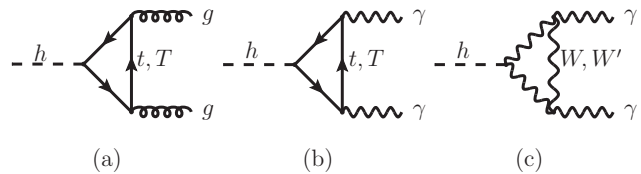


FIG. 2. The Feynman diagrams on the Higgs gluon gluon process (a) and Higgs to diphoton process (b,c).

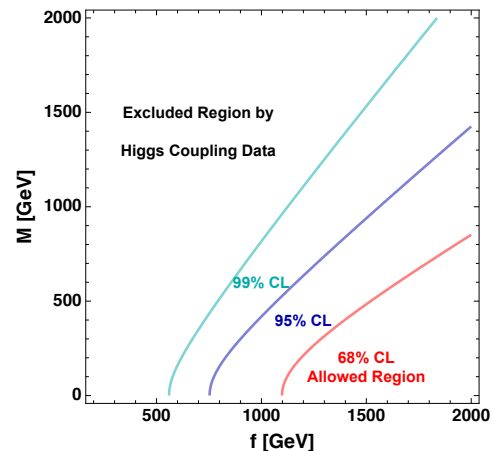


FIG. 3. The allowed contours on  $(f, M)$  at 68%, 95%, 99% CLs, according to the global fitting of the Higgs coupling data.

Although adding new scalars could lower the scale  $f$ , the Higgs coupling measurements will constrain the scale  $f$  whatever the new scalars exist or not. Independent of the new scalar sector, the Higgs coupling measurements put strong limit on the model parameters  $(f, M)$ . It is known that the Goldstone boson nature of the Higgs boson modifies the Higgs couplings to the SM gauge boson and SM fermions by a factor  $(1 - \frac{v^2}{f^2})$ . Furthermore, due to the mixing between  $t$  and  $T$ , the  $htt$  and  $hTT$  couplings are further modified by the mixing angle. This will affect the Higgs couplings to the gluon fields via the loop effects, as shown in Fig. 2(a). Finally, due to the existence of the charged gauge bosons and charged inert scalars, the Higgs diphoton couplings are also modified, as shown in Fig. 2(b,c). In principle, all the charged particles should be involved in the diphoton loop. Given that the masses of the  $H'_{L,R}^\mp$  depend on the soft mass terms, here for simplicity, we assume the  $H'_{L,R}^\mp$  are heavy, and thus the scalar contribution is negligible, compared to other contributions.

<sup>4</sup> Although the electroweak precision test might provide constraints on the mixing angle  $s_L$  and  $s_R$  between  $t$  and  $T$  for a sub-TeV  $T$  [39], the  $\mathbb{T}$ -parity between  $T$  and  $T'$  could weaken the electroweak precision constraints.

The relevant Higgs couplings are

$$\begin{aligned} hWW &: \frac{1}{2}g^2v \left(1 - \frac{v^2}{f^2}\right), & hW'W' &: -\frac{1}{2}g^2v \left(1 - \frac{v^2}{f^2}\right), \\ htt &: -\frac{y_t}{\sqrt{2}}c_Lc_R, & hTT &: -\frac{y}{\sqrt{2}}(s_Ls_R - c_Lc_R\frac{v}{f}), \end{aligned} \quad (51)$$

where  $s_L$  and  $s_R$  are mixing angle between  $t$  and  $T$ , defined in Eq. 72 in Appendix. Using these couplings, we calculate various Higgs signal strengths  $\mu_{pp \rightarrow h_1 \rightarrow ii} = \sigma(pp \rightarrow h_1)\text{Br}_{h_1 \rightarrow ii}/\sigma_{\text{SM}}\text{Br}_{\text{SM}}$ . Based on Higgs signal strengths at the 8 TeV LHC with  $20.7 \text{ fb}^{-1}$  data [40, 41], we perform a global fit on the model parameters. Fig. 3 shows the allowed contours on  $(f, M)$  at 68%, 95%, 99% CLs. Depending on values of the mass parameter  $M$ , the scale  $f$  could be as low as 750 GeV at 95% CL. As shown in the next section, the mass parameter  $M$  determines the mass scale of the  $\mathbb{T}$ -odd top partner  $T'$ . Given the current limit on the  $T'$  mass  $m_{T'} > 0.9 \text{ TeV}$ , we determine the scale  $f$  should be around 1.4 TeV at 95% CL.

## VI. $\mathbb{T}$ -ODD PARTICLE PHENOMENOLOGY

Unlike the  $\mathbb{T}$ -even particles, the signatures of the  $\mathbb{T}$ -odd particles provide very distinct features from the original twin Higgs model. Due to the exact  $\mathbb{T}$  parity, the  $\mathbb{T}$ -odd particles do not mix with the  $\mathbb{T}$ -even particles. Similar to the little Higgs models with  $\mathbb{T}$  parity [26, 27], we assign the  $\mathbb{T}$ -odd particles belong to dark sector, and the lightest  $\mathbb{T}$ -odd particle (LTP) is the dark matter candidate.

In this  $\mathbb{T}$ -parity twin Higgs setup, the  $\mathbb{T}$ -odd particles are the dark gauge boson  $B'$ , the dark top  $T'$  and all the component fields in  $H'$ . The  $\mathbb{T}$ -odd particle masses are  $m_{T'} = M$ , and  $m_{B'} = \frac{1}{2}g'f$ . As discussed above, the masses of the  $H'$  strongly depend on the soft mass terms, and typically  $m_{H'_{L,R}^{\pm}} \sim \lambda f^2$ ,  $m_{H'_{L,R}^0} \sim m_{A'_{L,R}^0} \sim m_{\text{soft}}$ . Depending on the soft mass term, the dark matter candidate could be either  $A'_{L,R}^0$  or the dark gauge boson  $B'$ . Here for simplicity, we assume the soft mass term, which is typically order of  $yf$ , is larger than  $gf$ , and take the dark gauge boson  $B'$  as the dark matter candidate. In this case, the dark matter signatures are quite different from the ones in the left-right twin Higgs model [31], which suggested the dark matter candidate is the neutral components of the inert Higgs.

Although the kinetic term of the dark gauge boson involves in  $H$ , there is no coupling between  $B'$  and the Higgs boson, such as  $B'B'hh$  and  $B'B'h$  terms. The  $B'$  typically interacts with the  $\mathbb{T}$ -odd  $T'$  via the  $\mathbb{T}$ -even top quarks, and couples to the  $H'_{L,R}^{\pm}$  and  $H'_{L,R}^0$  and electroweak gauge bosons. Therefore, the dominant dark matter annihilation processes are

- $B'B' \rightarrow W^+W^-/ZZ$  via  $t$ -channel exchange of  $H_L^{\pm}(H_L^0)$ ;
- $B'B' \rightarrow t\bar{t}$  via  $t$ -channel exchange of  $T'$ .

Since we have assumed the  $H_L^{\pm}(H_L^0)$  are heavy, the  $B'B' \rightarrow W^+W^-/ZZ$  process is suppressed compared to the  $B'B' \rightarrow t\bar{t}$  process. Thus it is very similar to the top flavored dark matter [42] with dark matter being vector boson. Unlike the fermionic top flavored dark matter, the  $t$ -channel process  $B'B' \rightarrow t\bar{t}$  provides us the  $s$ -wave component of the dark matter annihilation without chirality suppressed. Approximately, the  $s$ -wave  $B'B' \rightarrow t\bar{t}$  annihilation cross section is written as

$$(\sigma v)_{B'B' \rightarrow t\bar{t}} \simeq \frac{2N_c g'^4 Y^2}{9\pi} \frac{m_{B'}^2}{(m_{B'}^2 + m_{T'}^2)^2}, \quad (52)$$

where  $N_c$  is the color factor and  $Y$  is the top quark charge under  $B'$ . Having known the value of  $g'$ , we could determine the relation between  $m_{B'} = \frac{1}{2}g'f$  and  $m_{T'} = M$  from the dark matter relic abundance measurements. If only the  $B'B' \rightarrow t\bar{t}$  channel is dominant, the thermal relic abundance  $\Omega_{\text{dm}}h^2 \simeq 0.12$  puts constraint on the parameters  $(m_{B'}, m_{T'})$ , as shown in Fig. 5.

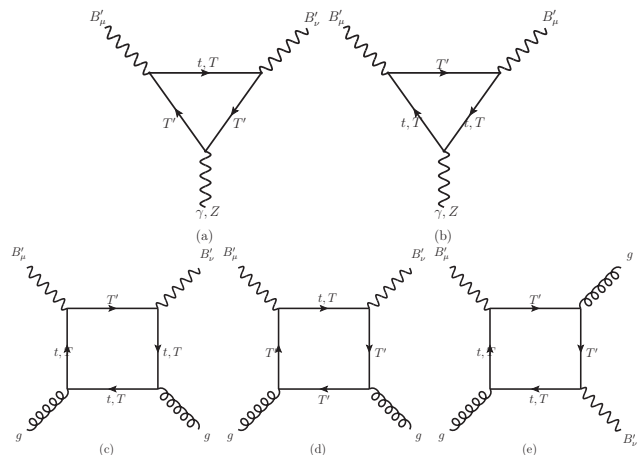


FIG. 4. The triangle (a,b) and box (c,d,e) Feynman diagrams which contribute to the dark matter direct detection.

We expect that the dark matter direct detection experiments will put further constraints on the model parameters. Because the  $B'$  does not couple to the Higgs boson, the dominant contributions to direct detection come from the one-loop triangle and box diagrams, similar to the studies in Ref. [43]. Let us calculate the low energy effective Lagrangian. According to Feynman diagrams shown in Fig. 4(a,b), the resulting effective Lagrangian is

$$\mathcal{L} = C_{\text{tri}} \epsilon^{\mu\nu\rho\sigma} (B'_\mu \partial_\nu B'_\rho) \bar{q} \gamma_\sigma \gamma_5 q, \quad (53)$$

where the Wilson coefficient  $C_{\text{tri}}$  is

$$\begin{aligned} C_{\text{tri}} \simeq N_c \frac{eQg'^2}{\pi^2} \frac{1}{6} \int_0^1 dz \frac{z^3}{m_t^2 + (m_{T'}^2 - m_t^2)z + m_{B'}^2 z(z-1)} \\ + (m_t \leftrightarrow m_{T'}). \end{aligned} \quad (54)$$

The box diagrams shown in Fig. 4(c,d,e) generate the following effective Lagrangian

$$\mathcal{L} = \alpha_s C_{\text{box}} B'^\rho B'_\rho G^{a\mu\nu} G_{\mu\nu}^a, \quad (55)$$

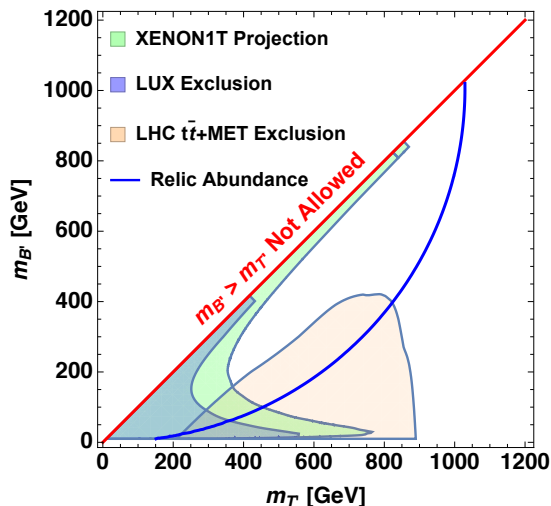


FIG. 5. The exclusion contours on the model parameters ( $m_{T'} = M, m_{B'} = \frac{1}{2}g'f$ ) by the LUX experiments, XENON1T projection, and the top pair plus transverse missing energy searches at the LHC. The blue line shows the prediction of the dark matter relic abundance if only the  $t$ -channel  $B'B' \rightarrow t\bar{t}$  is dominant.

where the Wilson coefficient  $C_{\text{box}}$  is approximately

$$C_{\text{box}} = \frac{g'^2}{48\pi} \frac{3m_{T'}^2 - 2m_{B'}^2}{(m_{T'}^2 - m_{B'}^2)^2}. \quad (56)$$

The triangle loop diagrams only contribute to the spin-dependent (SD) cross section, while the box loop diagrams contribute to the spin-independent (SI) cross section:

$$\begin{aligned} \sigma_N^{\text{SI}} &= \frac{\mu_N^2}{\pi} \left( \frac{4}{9} f_{TG}^{(N)} \frac{m_N}{m_{B'}} C_{\text{tri}} \right)^2, \\ \sigma_N^{\text{SD}} &= \frac{16\mu_N^2}{\pi} \left( e \sum_q \Delta_q^N C_{\text{box}} \right)^2, \end{aligned} \quad (57)$$

where  $f_{TG}^{(N)}$  and  $\Delta_q^N$  are defined in the Appendix of Ref. [43]. Then we utilize the complete exposure of the LUX 2016 data [44] to constrain the dark matter spin-independent (SI) cross section. We found that the exclusion limit is quite weak, as shown in Fig. 5. Then we also use the projected exclusion reach of the XENON1T experiment with an exposure of 2.2 ton years [45] to see whether the parameter region could be excluded by future experiments. Fig. 5 shows that the dark matter direct detection could not impose strong constraints on the model parameters.

On the other hand, the collider searches put stronger limits on these  $\mathbb{T}$ -odd particles. The  $\mathbb{T}$ -odd  $T'$  should have large production cross section because of the QCD production mechanism, and then subsequently decay to the top quark and the dark matter  $B'$ :

$$pp \rightarrow T'\bar{T}' \rightarrow tB'\bar{t}B', \quad (58)$$

which appears as the top quark pair plus transverse missing energy final states. This final states have been investigated at the LHC by both ATLAS [46] and CMS [47]. Although the LHC searches on this final states focus on the exclusion limit on the stop quark, it shares the same event topology as the  $\mathbb{T}$ -odd  $T'$  searches. Thus we could utilize the LHC exclusion limits on the stop quark, and recast the results of the exclusion limits into the exclusion limit of the  $\mathbb{T}$ -odd  $T'$  mass. To recast the exclusion limit, we assume the same cut efficiency in these processes and perform a simple scaling of the NNLO cross section of the stop quark to the NNLO cross section of the vectorlike top quark [48, 49]. We use the ATLAS analysis on stop quark searches with  $20.3 \text{ fb}^{-1}$  integrated luminosity at 8 TeV [46], and obtain the exclusion limit on  $(m_{T'}, m_{B'})$ , as shown in Fig. 5. From Fig. 5, we note that exclusion limit from the collider searches put much tighter constraints on the model parameters than the direct detection constraints. Combined all the constraints from Fig. 5 and Fig. 3 together, we find that the mass parameter  $M$  needs to be greater 900 GeV by the collider searches and at the same time the scale  $f$  needs to be greater than 1.4 TeV via the Higgs coupling measurements. According to Eq. 45, this corresponds to around 10% tuning.

Finally, the collider searches should also provide constraints on the  $\mathbb{T}$ -odd  $H'$ . Since  $m_{H'} > m_{B'} \sim 400$  GeV, we expect that mass of the  $H'$  should be heavier than 400 GeV. We know that typically the electroweak production limit is around 400 GeV. So compared to the limits from the  $T'$  searches and the Higgs coupling measurements, the current exclusion limit on the  $m_{H'}$  searches will not provide additional constraints. But we expect that the future searches on  $H'$  might be able to put constraints on the model parameters.

## VII. SUMMARY AND DISCUSSION

We have investigated implementing the  $\mathbb{T}$ -parity in the twin Higgs scenarios. This provides us a whole new sector, the  $\mathbb{T}$ -odd hidden sector and a promising dark matter candidate. We focused on one specific realization of this new scenario: the  $\mathbb{T}$ -parity extension of the left-right twin Higgs model. In this model, we discussed collider constraints on the  $\mathbb{T}$ -even particles, and dark matter phenomenology of the  $\mathbb{T}$ -odd sector. We found that the tightest constraints come from the combination of the Higgs coupling measurements and the  $\mathbb{T}$ -odd top partner searches at the LHC.

This  $\mathbb{T}$  parity twin Higgs model could be generalized to construct new kinds of twin Higgs models. And the interplay between the  $\mathbb{T}$  parity and the  $\mathbb{Z}_2$  symmetry might generate new ideas on the twin Higgs models. For example, we might be able to construct a theory in which the  $\mathbb{Z}_2$  symmetry only effects in the Higgs sector, but the  $\mathbb{T}$ -parity doubles the mass spectra. The further studies of this  $\mathbb{T}$  parity in twin Higgs model are under way. Over-

all, the implementation of the  $\mathbb{T}$  parity in the twin Higgs model might provide a new approach to understand the twin Higgs scenarios.

### ACKNOWLEDGMENTS

This work was supported by DOE Grant DE-SC0011095.

### APPENDIX: MASS MATRIX DIAGONALIZATION

Let us calculate the gauge boson masses. The  $\mathbb{T}$ -even charged gauge boson masses are

$$m_W^2 = \frac{1}{2}g^2 f^2 \sin^2 x, m_{W'}^2 = \frac{1}{2}g'^2 f^2 \cos^2 x, \quad (59)$$

where  $x = v/f$ . The  $\mathbb{T}$ -even neutral gauge bosons are mixed together. Their mass matrix is written as

$$\left( \begin{array}{c|ccc} & W_L^3 & W_R^3 & B \\ \hline W_L^3 & \frac{1}{2}g^2 f^2 \sin^2 x & 0 & -\frac{1}{2}gg' f^2 \sin^2 x \\ W_R^3 & 0 & \frac{1}{2}g'^2 f^2 \cos^2 x & -\frac{1}{2}gg' f^2 \cos^2 x \\ B & -\frac{1}{2}gg' f^2 \sin^2 x & -\frac{1}{2}gg' f^2 \cos^2 x & \frac{1}{2}g'^2 f^2 \end{array} \right). \quad (60)$$

Let us define the coupling constants

$$g = \frac{e}{s_w}, g' = \frac{e}{\sqrt{c_w^2 - s_w^2}} = \frac{e}{c_{2w}}, g_Y = \frac{e}{c_w}, \quad (61)$$

with the weak mixing angle defined as  $s_w = \sin \theta_w$  and  $c_w = \cos \theta_w$ . It is more convenient to work in the basis  $(A, Z_L, Z_R)$ , where

$$\begin{pmatrix} A \\ Z_L \\ Z_R \end{pmatrix} = \begin{pmatrix} s_w & s_w & \sqrt{c_{2w}} \\ -c_w & s_w t_w & t_w \sqrt{c_{2w}} \\ 0 & -\frac{\sqrt{c_{2w}}}{c_w} & t_w \end{pmatrix} \begin{pmatrix} W_L^3 \\ W_R^3 \\ B \end{pmatrix}. \quad (62)$$

In this basis, the mass eigenvalue of the gauge boson  $A$  is identically zero. We identify this gauge boson  $A$  is the photon that should remain massless after symmetry breaking. In this basis, the mass matrix reduces to

$$\left( \begin{array}{c|ccc} & A & Z_L & Z_R \\ \hline A & 0 & 0 & 0 \\ Z_L & 0 & M_{LL}^2 & M_{LR}^2 \\ Z_R & 0 & M_{LR}^2 & M_{RR}^2 \end{array} \right), \quad \text{with} \quad \begin{aligned} M_{LL}^2 &= \frac{g^2 + g_Y^2}{2} f^2 \sin^2 x, \\ M_{LR}^2 &= \frac{g_Y \sqrt{2g'^2 - g_Y^2}}{2} f^2 \sin^2 x, \\ M_{RR}^2 &= \frac{g^2 + g'^2}{2} f^2 - \frac{g^2 + g_Y^2}{2} f^2 \sin^2 x. \end{aligned} \quad (63)$$

The exact eigenstates  $Z, Z'$  are obtained via the rotation

$$\begin{pmatrix} Z \\ Z' \end{pmatrix} = \begin{pmatrix} \cos \vartheta & \sin \vartheta \\ -\sin \vartheta & \cos \vartheta \end{pmatrix} \begin{pmatrix} Z_L \\ Z_R \end{pmatrix}, \quad \tan 2\vartheta = \frac{2M_{LR}^2}{M_{LL}^2 - M_{RR}^2}. \quad (64)$$

The eigenvalues  $M_Z^2$  and  $M_{Z'}^2$  are given by

$$M_{Z,Z'}^2 = \frac{1}{2} \left( M_{LL}^2 + M_{RR}^2 \mp (M_{RR}^2 - M_{LL}^2) \sqrt{1 + \tan^2 2\vartheta} \right). \quad (65)$$

and approximately we have

$$M_Z^2 = M_{LL}^2 - \frac{M_{LR}^4}{M_{RR}^2 - M_{LL}^2}, \quad M_{Z'}^2 = M_{RR}^2 + \frac{M_{LR}^4}{M_{RR}^2 - M_{LL}^2}. \quad (66)$$

For the top quark sector, the Yukawa terms can be rewritten as

$$-\mathcal{L}_{\text{top}} = \begin{pmatrix} t_L \\ T_L \end{pmatrix} \begin{pmatrix} 0 & yH_R \\ yH_L & M \end{pmatrix} \begin{pmatrix} t_R \\ T_R \end{pmatrix}. \quad (67)$$

This gives rise to the following mass matrix squared

$$\mathcal{M}_{\text{top}}^2 = \begin{pmatrix} y^2 H_L^\dagger H_L & yMH_L \\ yMH_L & M^2 + y^2 H_R^\dagger H_R \end{pmatrix}. \quad (68)$$

Defining the mass eigenstates

$$\begin{pmatrix} t_{L,R}^{\text{mass}} \\ T_{L,R}^{\text{mass}} \end{pmatrix} = \begin{pmatrix} \cos \alpha_{L,R} & \sin \alpha_{L,R} \\ -\sin \alpha_{L,R} & \cos \alpha_{L,R} \end{pmatrix} \begin{pmatrix} t_{L,R} \\ T_{L,R} \end{pmatrix}, \quad \tan 2\alpha_{L,R} = \frac{4yMH_{R,L}}{M^2 + y^2 H_{L,R}^2 - y^2 H_{R,L}^2}, \quad (69)$$

we could diagonalize the mass matrix squared, and obtain the mass eigenstates

$$m_{t,T}^2 = \frac{1}{2}(M^2 + y^2 f^2 \mp \sqrt{(M^2 + y^2 f^2)^2 - y^4 f^4 \sin^2 2x}). \quad (70)$$

The mixing angles are

$$\sin \alpha_L = \sqrt{1 - (y^2 f^2 \cos 2x + M^2) / \sqrt{(M^2 + y^2 f^2)^2 - y^4 f^4 \sin^2 2x}}, \quad (71)$$

$$\sin \alpha_R = \sqrt{1 - (y^2 f^2 \cos 2x - M^2) / \sqrt{(M^2 + y^2 f^2)^2 - y^4 f^4 \sin^2 2x}}. \quad (72)$$

- 
- [1] Z. Chacko, H. S. Goh and R. Harnik, Phys. Rev. Lett. **96**, 231802 (2006); JHEP **0601**, 108 (2006).  
[2] Z. Chacko, H. S. Goh and R. Harnik, JHEP **0601**, 108 (2006) [hep-ph/0512088].  
[3] A. Falkowski, S. Pokorski and M. Schmaltz, Phys. Rev. D **74**, 035003 (2006) doi:10.1103/PhysRevD.74.035003 [hep-ph/0604066].  
[4] S. Chang, L. J. Hall and N. Weiner, Phys. Rev. D **75**, 035009 (2007) doi:10.1103/PhysRevD.75.035009 [hep-ph/0604076].  
[5] N. Craig and K. Howe, JHEP **1403**, 140 (2014) doi:10.1007/JHEP03(2014)140 [arXiv:1312.1341 [hep-ph]].  
[6] N. Craig, S. Knapen and P. Longhi, Phys. Rev. Lett. **114**, no. 6, 061803 (2015); JHEP **1503**, 106 (2015).  
[7] M. Geller and O. Telem, Phys. Rev. Lett. **114**, 191801 (2015) doi:10.1103/PhysRevLett.114.191801 [arXiv:1411.2974 [hep-ph]].  
[8] R. Barbieri, D. Greco, R. Rattazzi and A. Wulzer, JHEP **1508**, 161 (2015) doi:10.1007/JHEP08(2015)161 [arXiv:1501.07803 [hep-ph]].  
[9] M. Low, A. Tesi and L. T. Wang, Phys. Rev. D **91**, 095012 (2015) doi:10.1103/PhysRevD.91.095012 [arXiv:1501.07890 [hep-ph]].  
[10] H. Beauchesne, K. Earl and T. Grgoire, JHEP **1601**, 130 (2016).  
[11] R. Harnik, K. Howe and J. Kearney, arXiv:1603.03772 [hep-ph].  
[12] J. H. Yu, Phys. Rev. D **94**, no. 11, 111704 (2016) doi:10.1103/PhysRevD.94.111704 [arXiv:1608.01314 [hep-ph]]; J. H. Yu, JHEP **1612**, 143 (2016) doi:10.1007/JHEP12(2016)143 [arXiv:1608.05713 [hep-ph]].  
[13] A. Katz, A. Mariotti, S. Pokorski, D. Redigolo and R. Ziegler, arXiv:1611.08615 [hep-ph].  
[14] G. Burdman, Z. Chacko, R. Harnik, L. de Lima and C. B. Verhaaren, Phys. Rev. D **91**, no. 5, 055007 (2015).  
[15] N. Craig, A. Katz, M. Strassler and R. Sundrum, JHEP **1507**, 105 (2015).  
[16] H. C. Cheng, S. Jung, E. Salvioni and Y. Tsai, JHEP **1603**, 074 (2016) [arXiv:1512.02647 [hep-ph]].  
[17] Z. Chacko, D. Curtin and C. B. Verhaaren, Phys. Rev. D **94**, no. 1, 011504 (2016) [arXiv:1512.05782 [hep-ph]].  
[18] N. Craig and A. Katz, JCAP **1510**, no. 10, 054 (2015) [arXiv:1505.07113 [hep-ph]].  
[19] I. Garca Garca, R. Lasenby and J. March-Russell, Phys.

- Rev. D **92**, no. 5, 055034 (2015) [arXiv:1505.07109 [hep-ph]]; Phys. Rev. Lett. **115**, no. 12, 121801 (2015) [arXiv:1505.07410 [hep-ph]].
- [20] M. Farina, JCAP **1511**, no. 11, 017 (2015) doi:10.1088/1475-7516/2015/11/017 [arXiv:1506.03520 [hep-ph]].
- [21] M. Freytsis, S. Knapen, D. J. Robinson and Y. Tsai, JHEP **1605**, 018 (2016) [arXiv:1601.07556 [hep-ph]].
- [22] V. Prilepina and Y. Tsai, arXiv:1611.05879 [hep-ph].
- [23] Z. Chacko, N. Craig, P. J. Fox and R. Harnik, [arXiv:1611.07975 [hep-ph]].
- [24] N. Craig, S. Koren and T. Trott, arXiv:1611.07977 [hep-ph].
- [25] P. Batra and Z. Chacko, Phys. Rev. D **79**, 095012 (2009) doi:10.1103/PhysRevD.79.095012 [arXiv:0811.0394 [hep-ph]].
- [26] H. C. Cheng and I. Low, JHEP **0309**, 051 (2003) [hep-ph/0308199].
- [27] H. C. Cheng and I. Low, JHEP **0408**, 061 (2004) [hep-ph/0405243].
- [28] H. Georgi, Nucl. Phys. B **266**, 274 (1986).
- [29] S. R. Coleman and E. J. Weinberg, Phys. Rev. D **7**, 1888 (1973). doi:10.1103/PhysRevD.7.1888
- [30] H. S. Goh and S. Su, Phys. Rev. D **75**, 075010 (2007).
- [31] E. M. Dolle and S. Su, Phys. Rev. D **77**, 075013 (2008) [arXiv:0712.1234 [hep-ph]].
- [32] CMS Collaboration [CMS Collaboration], CMS-PAS-B2G-16-017.
- [33] G. Aad *et al.* [ATLAS Collaboration], Phys. Lett. B **743**, 235 (2015) [arXiv:1410.4103 [hep-ex]].
- [34] V. Khachatryan *et al.* [CMS Collaboration], [arXiv:1609.05391 [hep-ex]].
- [35] The ATLAS collaboration [ATLAS Collaboration], ATLAS-CONF-2016-045.
- [36] The ATLAS collaboration [ATLAS Collaboration], ATLAS-CONF-2016-102.
- [37] S. Chatrchyan *et al.* [CMS Collaboration], Phys. Lett. B **729**, 149 (2014) [arXiv:1311.7667 [hep-ex]].
- [38] K. Hsieh, K. Schmitz, J. H. Yu and C.-P. Yuan, Phys. Rev. D **82**, 035011 (2010) [arXiv:1003.3482 [hep-ph]].
- [39] M. L. Xiao and J. H. Yu, Phys. Rev. D **90**, no. 1, 014007 (2014) Addendum: [Phys. Rev. D **90**, no. 1, 019901 (2014)] [arXiv:1404.0681 [hep-ph]].
- [40] G. Aad *et al.* [ATLAS Collaboration], Eur. Phys. J. C **76**, no. 1, 6 (2016);
- [41] V. Khachatryan *et al.* [CMS Collaboration], Eur. Phys. J. C **75**, no. 5, 212 (2015).
- [42] C. Kilic, M. D. Klimek and J. H. Yu, Phys. Rev. D **91**, no. 5, 054036 (2015) [arXiv:1501.02202 [hep-ph]].
- [43] J. H. Yu, Phys. Rev. D **90**, no. 9, 095010 (2014) [arXiv:1409.3227 [hep-ph]].
- [44] D. S. Akerib *et al.*, arXiv:1608.07648 [astro-ph.CO].
- [45] E. Aprile [XENON1T Collaboration], Springer Proc. Phys. **148**, 93 (2013) [arXiv:1206.6288 [astro-ph.IM]].
- [46] G. Aad *et al.* [ATLAS Collaboration], Eur. Phys. J. C **75**, no. 10, 510 (2015) Erratum: [Eur. Phys. J. C **76**, no. 3, 153 (2016)] doi:10.1140/epjc/s10052-015-3726-9, 10.1140/epjc/s10052-016-3935-x [arXiv:1506.08616 [hep-ex]].
- [47] V. Khachatryan *et al.* [CMS Collaboration], Eur. Phys. J. C **76**, no. 8, 460 (2016) doi:10.1140/epjc/s10052-016-4292-5 [arXiv:1603.00765 [hep-ex]].
- [48] M. Aliev, H. Lacker, U. Langenfeld, S. Moch, P. Uwer and M. Wiedermann, Comput. Phys. Commun. **182**, 1034 (2011) doi:10.1016/j.cpc.2010.12.040 [arXiv:1007.1327 [hep-ph]].
- [49] D. Goncalves-Netto, D. Lopez-Val, K. Mawatari, T. Plehn and I. Wigmore, Phys. Rev. D **87**, no. 1, 014002 (2013) doi:10.1103/PhysRevD.87.014002 [arXiv:1211.0286 [hep-ph]].